

The effects of topography on local wind-induced pressures of a medium-rise building

P.A. Hitchcock^{*1}, K.C.S. Kwok², K.S. Wong¹ and K.M. Shum¹

¹CLP Power Wind/Wave Tunnel Facility,
The Hong Kong University of Science and Technology, Hong Kong SAR

²School of Engineering, University of Western Sydney, Australia

(Received June 26, 2009, Accepted March 6, 2010)

Abstract. Wind tunnel model tests were conducted for a residential apartment block located within the complex terrain of The Hong Kong University of Science and Technology (HKUST). The test building is typical of medium-rise residential buildings in Hong Kong. The model study was conducted using modelling techniques and assumptions that are commonly used to predict design wind loads and pressures for buildings sited in regions of significant topography. Results for the building model with and without the surrounding topography were compared to investigate the effects of far-field and near-field topography on wind characteristics at the test building site and wind-induced external pressure coefficients at key locations on the building façade. The study also compared the wind tunnel test results to topographic multipliers and external pressure coefficients determined from nine international design standards. Differences between the external pressure coefficients stipulated in the various standards will be exacerbated when they are combined with the respective topographic multipliers.

Keywords: wind-induced pressure; medium-rise building; topography; wind tunnel; international design standards and codes of practice.

1. Introduction

For the majority of low-rise and medium-rise buildings, the definition of which is likely to vary internationally (Uematsu and Isyumov 1999, Letchford *et al.* 2005), it is typical that wind-induced pressures and loads will be predicted using a design standard, or code of practice procedure, that is based on a quasi-steady approach. In general, quasi-steady procedures treat separately the elements of determining the wind characteristics relevant to a particular site and the aerodynamic characteristics of the structure to be designed, where the latter are based on test results for isolated buildings. Several recent publications (Zhang 2003, St. Pierre *et al.* 2005, Holmes *et al.* 2005, Letchford *et al.* 2005, Holmes 2007) have assessed and compared wind loading provisions in international design standards and codes. In their review of major international standards and codes, Letchford *et al.* (2005) noted a number of discrepancies related to wind loads and pressures on low-rise buildings, from regional peculiarities to substantial differences in the

* Corresponding Author, Associate Director, E-mail: wtpete@ust.hk

loading coefficients. Holmes *et al.* (2005) reviewed aspects related to wind structure, i.e., terrain/exposure type, shielding, shelter and interference, and topographic effects, and noted significant differences particularly in relation to calculating topographic multipliers. Given the variations in the individual design parameters, it is to be expected that combinations of those parameters will also result in large differences between design loads predicted by the various international standards and codes.

This paper reports wind tunnel model test results for a residential, medium-rise apartment block located within the campus of The Hong Kong University of Science and Technology (HKUST). The study used modeling techniques and assumptions that are commonly employed to predict design wind pressures for buildings sited in regions of significant topography, to investigate the effects of the topography on external wind pressures acting at locations of interest on the building façade. The paper also compares the wind tunnel model test results with various international design standards and codes of practice, in particular the topographic multipliers and mean external pressure coefficients at specific locations of interest on the windward, side and leeward faces of the test building.

2. The HKUST test building

The Hong Kong University of Science and Technology (HKUST) is situated on the east coast of the Kowloon peninsula amidst complex terrain. Campus buildings are generally low-rise to medium-rise, i.e., of the order of 3 – 12 storeys, and all are located on a hillside facing approximately north-east that extends from the seafront to approximately 120 m above sea level. The HKUST test building is one of a pair of residential towers located towards the top of the hillside (108 m above sea level) and has plan dimensions of 16.6 m × 30.6 m and an overall height of 30.4 m above the adjacent ground level. The hillside in front of the test building slopes steeply down to the waterfront at an angle of approximately 26° to the horizontal, i.e., with an average slope of approximately 0.48. The terrain immediately behind the test building slopes uphill with a gradient of approximately 0.2 for a short distance, before reducing to a mild uphill slope with an average gradient of approximately 0.05.

A 1:400 scale model of the test building was installed with 102 pressure-taps, as indicated in Fig. 1, that were mounted flush with the model surfaces, and connected to a high-frequency pressure scanner system via flexible tubing. The pressure taps were installed at window and corner locations on the walls of the model and arranged in three layers coinciding with the 5th, 7th and 8th floors of the test building, where the 8th floor is the highest occupied level. The study focused on locations on the 7th floor where there are openable windows, including the north-east windward face (pressure-taps 726 and 728), the north-west side face (pressure-tap 729) and the south-west leeward face (pressure-tap 709). An additional pressure-tap was included close to the corner of the north-west side face (pressure-tap 7004) to provide measurements that are representative of typical edge zones.

3. Assessment of the effects of far-field topography

The HKUST test building has a relatively open exposure to incident winds from the north-east quadrant, i.e., 0° to 90° from north, with a mix of open water fetches and isolated islands, as shown

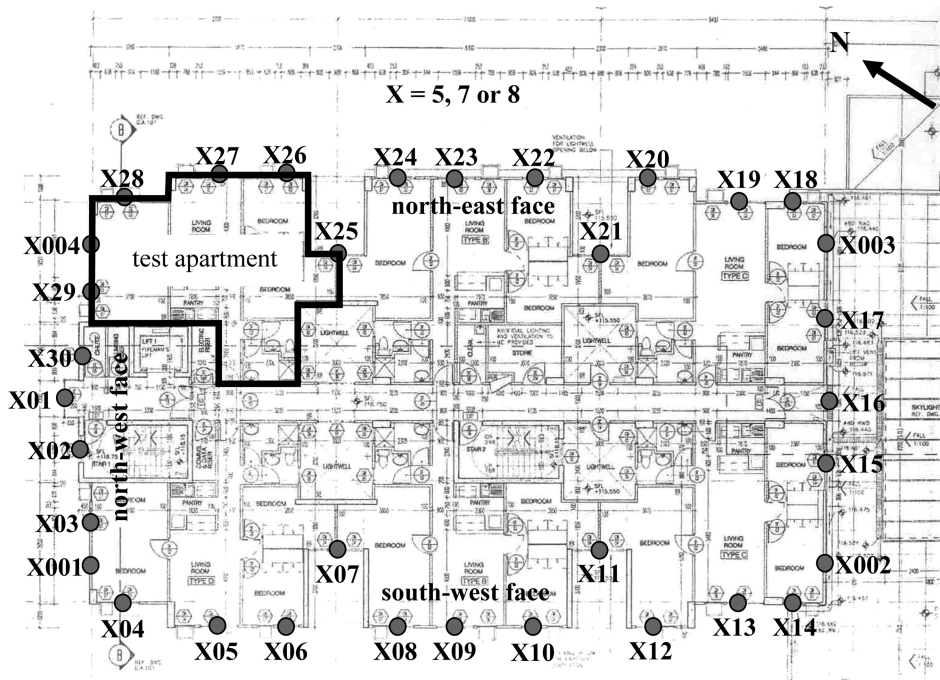


Fig. 1 Plan view of the HKUST test building and pressure-tap layout (prefix X represents the floor number, where X = 5, 7 or 8)

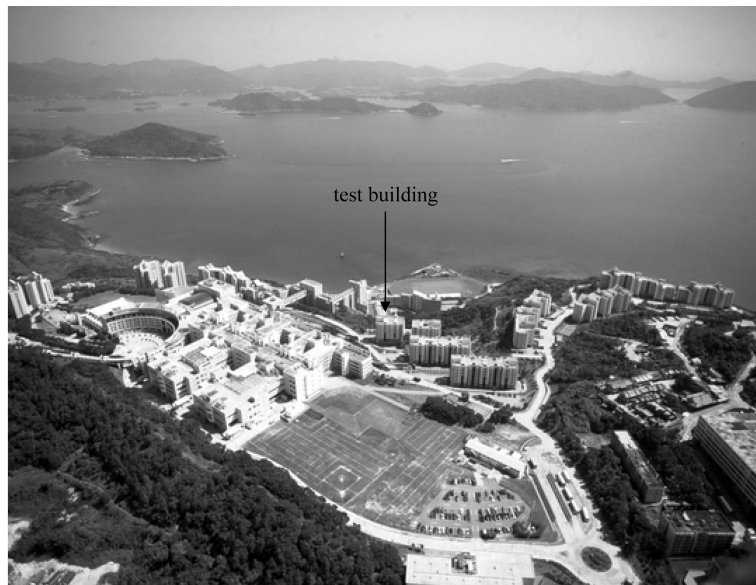


Fig. 2 Northeast exposure of the HKUST test building

in Fig. 2. Although a number of researchers (Miller and Davenport 1998, Weng *et al.* 2000, Kondo *et al.* 2002) have proposed guidelines, it is not straightforward to accurately assess the effects of the

type of non-uniform far-field topography that is often encountered in coastal areas in Hong Kong, without the benefit of some form of physical model measurement or computational simulation of wind flow. For the current study, the effects of the far-field topography were measured in a wind tunnel topography study using a model scale of 1:2000 to include the surrounding area within a 10 km radius from the test building site. Mountains and hills were modeled at 20 m contour intervals, in a terraced arrangement to provide the model with a “rough” surface in accordance with the findings of other researchers (Glanville and Kwok 1997, Chock and Cochran 2006). Relatively detailed models of all buildings within a radius of approximately 1 km from the test building were included in the 1:2000 scale model, and less detailed models were used to simulate buildings beyond that distance. Winds approaching the modeled region in the 1:2000 scale study were scaled to simulate typhoon wind characteristics stipulated in the Code of Practice on Wind Effects in Hong Kong (Buildings Department 2004), as shown in Figs. 3 and 4.

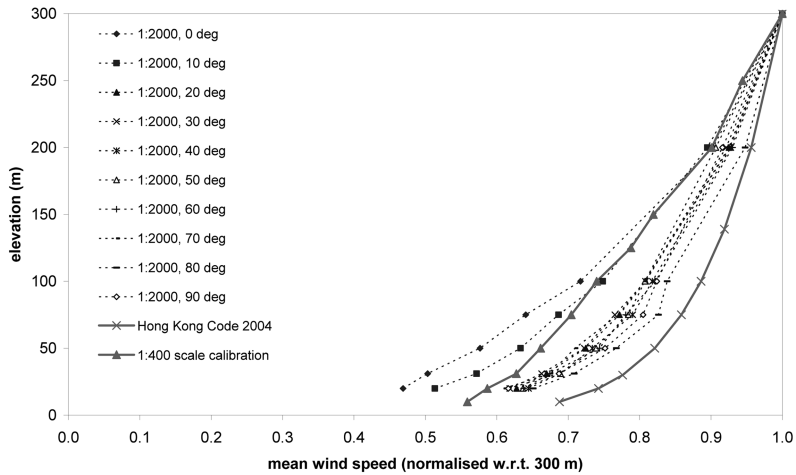


Fig. 3 Mean wind speed profiles

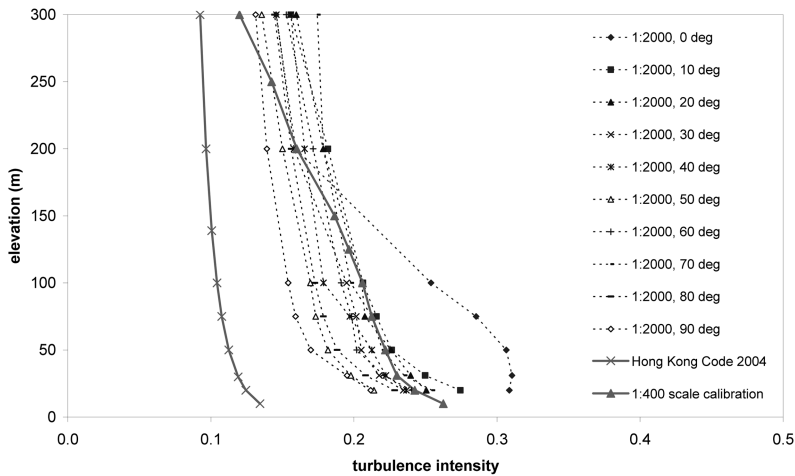


Fig. 4 Turbulence intensity profiles

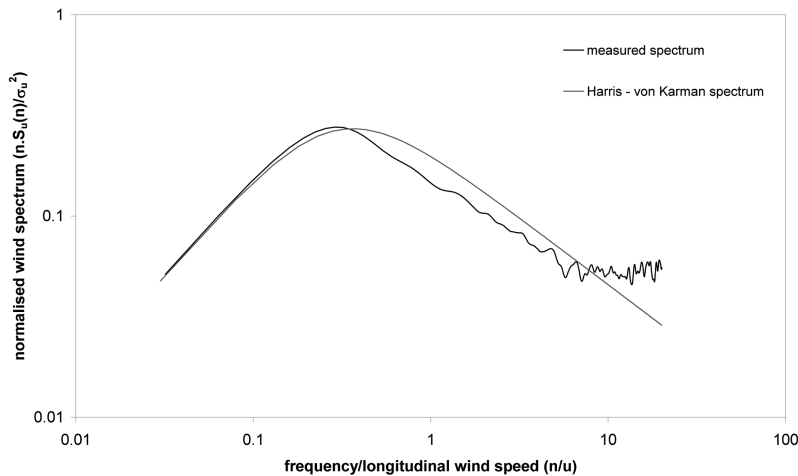


Fig. 5 Spectrum of longitudinal wind speed at building height (30 m), turbulence length scale = 160 m

Measurements of wind speed and turbulence intensity were taken at a distance of approximately 500 m upstream of the test building site, i.e., above the nominal water surface and slightly upstream of the hillside, to be consistent with the extent of the proximity model that was used in subsequent 1:400 scale model tests. Measurements were taken using a series 100 dynamic Cobra probe, manufactured by Turbulent Flow Instrumentation Pty. Ltd., at 10° intervals ranging from north (0°) to east (90°) inclusive, at seven heights. The measured directional profiles of mean wind speed and turbulence intensity are also presented in Figs. 3 and 4. It can be seen from Figs. 3 and 4 that the approaching wind was significantly affected by the far-field terrain, with significant reductions in the mean wind speed and corresponding increases in the turbulence intensity.

One representative approach flow was simulated at a scale of 1:400, for use in subsequent pressure model tests, using combinations of floor roughness and turbulence generators spanning the full width of the wind tunnel test section. Profiles of mean wind speed and turbulence intensity that were used for the 1:400 scale model studies are also presented in Figs. 3 and 4, and the corresponding spectrum of the longitudinal wind speed at a height equivalent to the top of the building (approximately 30 m) is presented in Fig. 5.

4. Assessment of the effects of near-field topography

4.1 Physical model

The effects of the topography and buildings within the HKUST campus were investigated quantitatively using a physical model that focused on incident winds perpendicular to the wide north-east face of the test building, i.e., an incident wind direction of 58° . The 1:400 scale model of the test building and the surrounding area had a radius of approximately 500 m and included the hillside and all existing buildings within the HKUST campus at the time of testing. The topography in the campus model was fabricated at 4 m contour intervals. The 1:400 scale model of the HKUST campus created a blockage ratio of less than 10%.

4.2 Boundary layer flow over the escarpment

Time histories of the three components of wind velocity were measured using a series 100 dynamic Cobra probe, manufactured by Turbulent Flow Instrumentation Pty. Ltd., along a longitudinal vertical plane parallel to the centerline of the wind tunnel. The measurement area started from a distance of 1.75 m upstream of the centre of the model and ended close to the top of the hillside in front of the test building, to investigate the development and modification of the wind speed and turbulence intensity profiles as the wind flowed up the hillside to the test building site. For all the wind velocity measurements, the model was oriented at an incident wind direction of 58° from north, so that the approaching wind was approximately normal to the wide north-east face of the test building and the vertical plane was aligned with the test building.

Profiles of mean longitudinal wind velocity and turbulence intensity along the measurement plane in the wind tunnel model are presented in Figs. 6 and 7 respectively. The presence of three student

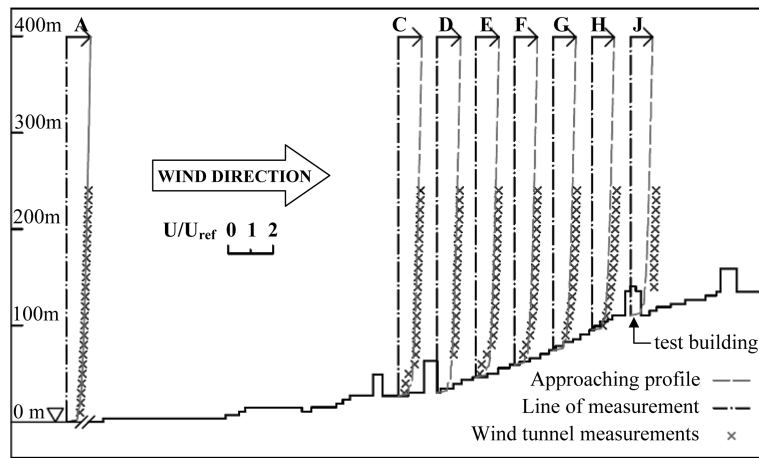


Fig. 6 Longitudinal velocity profiles along the measurement plane

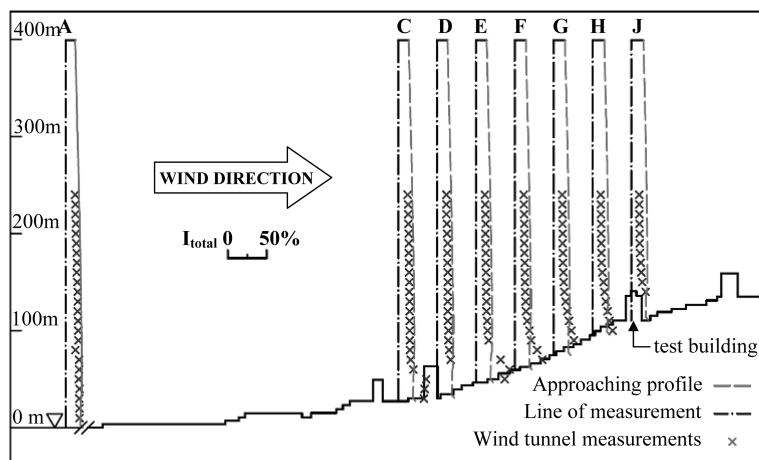


Fig. 7 Total turbulence intensity profiles along the measurement plane

residential buildings at the bottom of the hillside initially disrupted the wind flow, causing significant increases in the magnitude of the turbulence intensity from ground level up to approximately 50 m above ground level, as shown at location C in Figs. 6 and 7. Similarly, significant lateral and vertical velocity components were introduced into the wind flow. Towards the crest of the escarpment, at location H, the turbulent effects of the student residences had dissipated significantly and the resultant velocity at a height of 30 m above ground level was effectively parallel to the slope of the topography, although there was an indication of enhanced lateral wind flow which is attributed to the commencement of diverging wind flow around the test building.

At location H in Fig. 6, the mean wind speed at a height of 30 m relative to the corresponding value at 30 m in the approach flow indicates that the mean topographic multiplier, as defined in Eq. (1), for the hillside has a magnitude of 1.3. This is of a similar magnitude to the mean topographic multiplier of 1.2 reported by Holmes *et al.* (1997) for an escarpment with a similar average slope.

$$\text{mean topographic multiplier} = \frac{\text{mean wind speed at height } z \text{ above the hillside}}{\text{mean wind speed at height } z \text{ above flat ground upwind}} \quad (1)$$

The magnitude of the turbulence intensity at building height was reduced from approximately 22% in the approaching wind flow to around 19% at location H.

5. Wind-induced external pressures

The 1:400 scale pressure model was tested in two configurations: 1) embedded in the surrounding model, which is designated as the ‘with topography’ test configuration; and 2) mounted directly on the wind tunnel floor with all surrounding topography and buildings removed, which is designated as the ‘without topography’ test configuration. Similar mean wind speed and turbulence intensity profiles were used for both test configurations and the turbulence intensity at building height in the approach flow was approximately 22-23%. For both test configurations, measurements were taken for a wind direction of 58° from grid north, i.e., for winds normal to the north-east face of the test building.

Surface wind pressures were transferred through a three stage restricted tubing system that was carefully designed to eliminate resonance effects, giving an effectively constant amplitude response and linear phase response up to almost 400 Hz. Beyond 400 Hz, the tubing system effectively acted as a pneumatic low-pass filter. Measurements of wind pressure were sampled at a rate of 600 Hz via pressure transducers of high-speed scanner modules located underneath the test building model. A 4th order, low-pass filter with a cut-off frequency of 150 Hz was subsequently applied to the measured surface pressures during post-processing of the test data.

For both test configurations, reference pressures were measured directly above the test building model at a height equivalent to 300 m above the local ground level, i.e., in a location of sufficiently low turbulence intensity and to avoid the effects of inclined wind flow that were induced by the topography upstream of the test building. The results for both test configurations were subsequently corrected to building height for both the ‘with topography’ and ‘without topography’ test configurations. Mean, standard deviation, maximum and minimum pressure coefficients were determined from time histories of instantaneous fluctuating surface pressures, in accordance with Eq. (2)

$$C_{p,j}(t) = \frac{p_j(t)}{q_h} \tag{2}$$

where $p_j(t)$ is the instantaneous fluctuating surface pressure at pressure-tap j at time t measured relative to the mean static pressure in the wind tunnel, q_h is the reference mean dynamic pressure ($q_h = 0.5\rho\bar{u}_h^2$), ρ is the density of air (taken as 1.205 kg/m^3 for this study) and \bar{u}_h is the mean wind speed at building height.

The largest magnitude positive (maximum) and largest magnitude negative (minimum) external wind pressure coefficients at each pressure tap location were determined as the average of the measured maximum and minimum external pressure coefficients from ten equal samples that were equivalent to approximately one hour each at prototype-scale.

Contours of mean pressure coefficients for the ‘without topography’ configuration are presented in Fig. 8 for the north-east, north-west and south-west building faces, for winds normal to the north-east face of the test building, i.e., 58° from north. It can be seen from Fig. 8 that the largest mean pressure coefficient measured on the windward north-east face of the ‘without topography’ test configuration was approximately 0.8 at pressure-tap 523, i.e., close to the middle of the windward

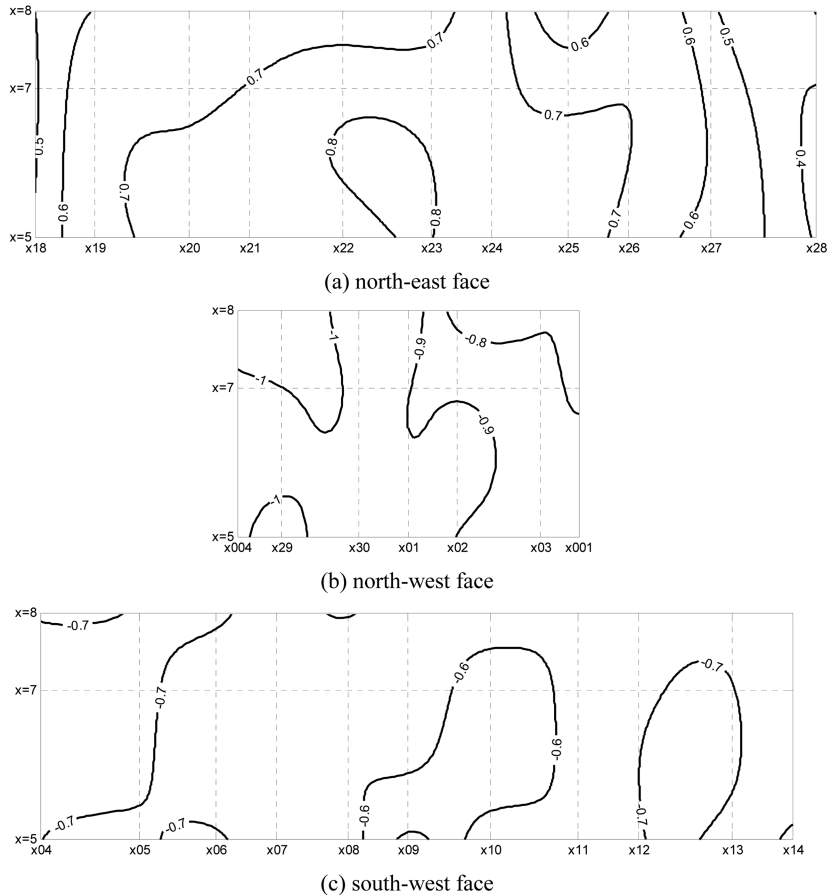


Fig. 8 Mean pressure coefficient contours, ‘without topography’

face and at approximately 60% of the overall building height. The distribution of mean pressure coefficients on the north-east face is asymmetrical due to the presence of the neighboring tower. The largest magnitude mean pressure coefficient on the north-west side face was approximately -1.1 close to the leading edge, decreasing to approximately -0.8 towards the downstream edge. The pressure coefficients measured on the leeward face were consistently of the order of -0.6 to -0.7. These magnitudes of mean pressure coefficient are consistent with those that would be typically expected for an isolated rectangular building with a flat roof.

Corresponding mean pressure coefficients for the ‘with topography’ test configuration are presented in Fig. 9. It is evident from a comparison of the mean pressure coefficients for the ‘without topography’ and ‘with topography’ configurations, that there are some differences in the overall pressure distributions, probably due to the effects of the topography and surrounding buildings, but that the magnitudes are quite similar for the two test configurations. Furthermore, the magnitudes of the maximum, minimum, mean and standard deviation external pressure coefficients for pressure-taps 726, 728, 7004, 729 and 709, summarized in Table 1, are quite similar for both ‘with topography’ and ‘without topography’ configurations.

Although the magnitudes of the minimum pressure coefficients for pressure-taps 7004 and 729 are

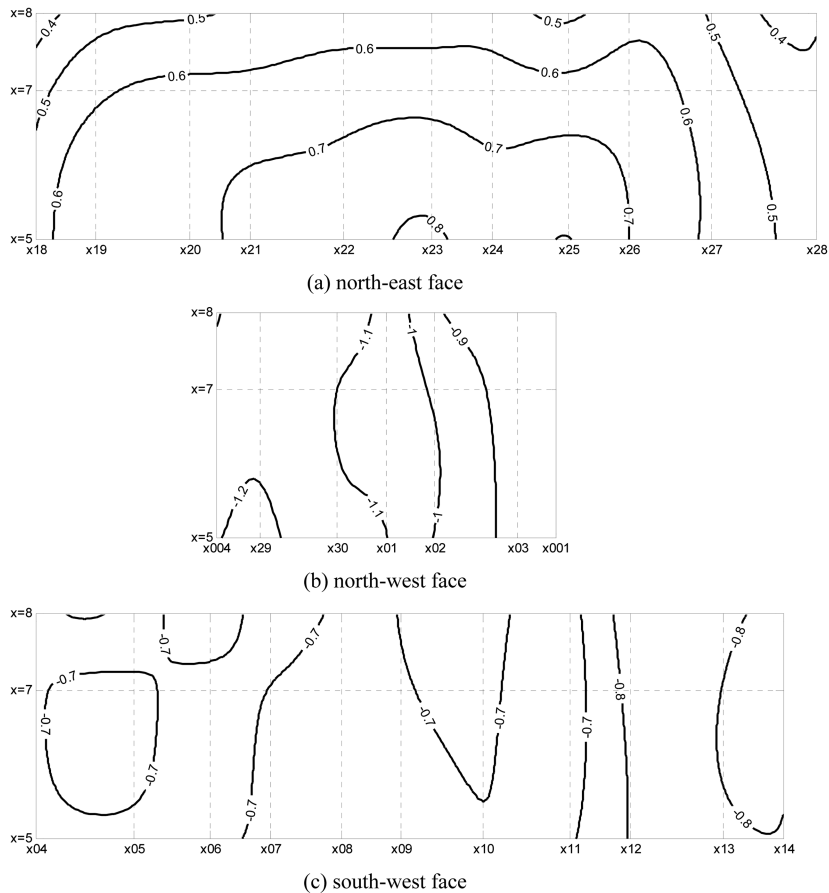


Fig. 9 Mean pressure coefficient contours, ‘with topography’

Table 1 Summary of external pressure coefficients

Pressure-tap	$C_{pe,max}$		$C_{pe,min}$		$C_{pe,mean}$		$C_{pe,std}$	
	‘Without topography’		‘Without topography’		‘Without topography’		‘Without topography’	
	‘With topography’		‘With topography’		‘With topography’		‘With topography’	
726 (windward wall- central)	2.4	2.9	-0.4	-0.4	0.6	0.7	0.4	0.7
728 (windward wall – edge)	2.3	2.8	-1.4	-1.6	0.4	0.4	0.5	0.4
7004 (side wall– edge zone)	0.0	0.1	-3.2	-3.7	-1.2	-1.0	0.4	0.4
729 (side wall)	0.2	0.4	-3.4	-3.8	-1.2	-1.0	0.4	0.5
709 (leeward wall)	0.0	0.0	-1.5	-1.8	-0.7	-0.7	0.2	0.2

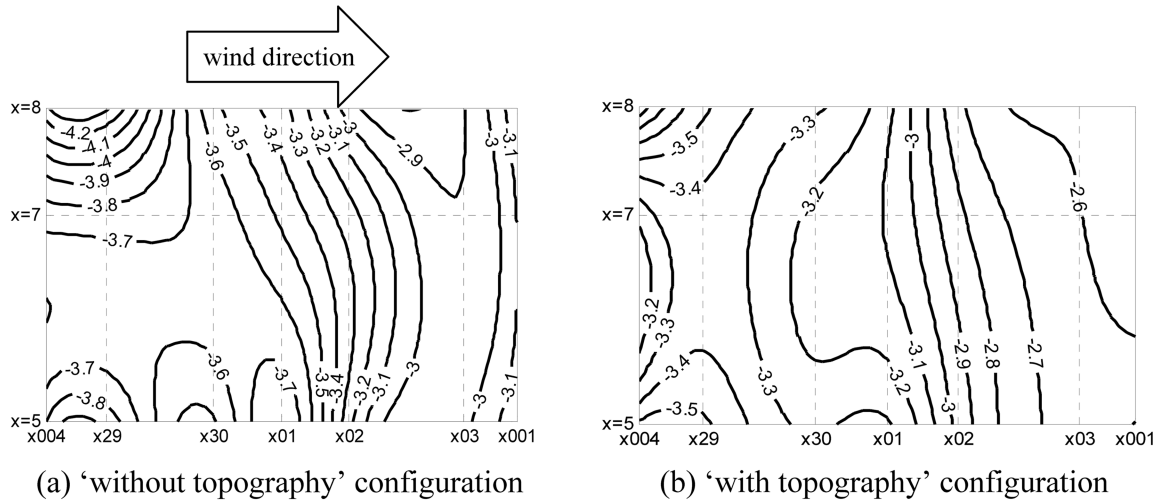


Fig. 10 Minimum pressure coefficient contours, north-west side face

similar in Table 1, it can be seen in Fig. 10 that the magnitudes of the minimum pressure coefficients over the north-west side face gradually decrease along the direction of the approaching wind. As expected, particularly high suction pressures were measured for both the ‘without topography’ and ‘with topography’ configurations in the vicinity of the top corner of the leading edge.

6. Comparison with international standards and codes of practice

International design standards and wind codes typically combine pressure coefficients based on quasi-steady assumptions with a topographic multiplier to predict peak design wind pressures on buildings in significant topography. For this study, topographic multipliers and external pressure coefficients were determined from nine international design standards and wind codes, including the Architectural Institute of Japan AIJ 2004 (2004); Australia/New Zealand Standard AS/NZS 1170.2:2002 (2002); American Society of Civil Engineers SEI/ASCE 7-05 (2005); British Standard BS 6399-2:1997 (2002); Eurocode 1 EN 1991-1-4:2005 (C.E.N. 2005); Code of Practice on Wind Effects in Hong Kong (Buildings Department 2004); Chinese National Standard GB 50009-2001 (2001); Indian Standard IS:875 (1987); and National Building Code of Canada NBCC 2005 (2005), for comparison with the wind tunnel test results.

In order to remove a number of the variables and discrepancies identified by Letchford *et al.* (2005) and Holmes *et al.* (2005), the following qualifications were made to ensure consistency between calculations and assumptions used in both the wind tunnel model studies and the various design standards:

1. the test building was classified as a rectangular building with a flat roof;
2. no shielding or sheltering was assumed;
3. wind directionality was not considered;
4. the near-field topography was assumed to be a two-dimensional escarpment for winds normal to the north-east building face;
5. the test building was assumed to be located at the crest of the escarpment;
6. the height of the test building is 30.35 m above the adjacent ground level;
7. all pressure coefficients were determined for wind normal to the north-east wide face of the test building, which is the most exposed of the four building faces.

6.1 Topographic multipliers

Each of the standards considered in this study include similar formulations for the design wind speed, such as that presented in Eq. (3), where the basic wind speed, v_0 , or pressure, is modified through the application of a number of multipliers to account for the effects of wind directionality, M_d , terrain type and height, M_z , shielding, M_s , topography, M_t , and structural importance or the level of risk or return period, M_R .

$$v_{des} = v_0 M_d M_z M_s M_t M_R \quad (3)$$

Basic design quantities for the aforementioned standards and codes are listed in Table 2. In each of the standards, the basic wind speeds or pressures are all given at a reference height of 10 m above flat, open terrain. AIJ 2004, BS 6399-2:1007, GB 50009-2001 and NBCC 2005 each use a mean basic wind speed or pressure, with corresponding averaging times of 10 min, 1 hour, 10 min

Table 2 Basic design quantities

Code/Standard	Country/Region	Basic wind quantity	Design wind quantity	Return period	Topographic multiplier
AIJ 2004	Japan	10 min mean speed, U_0	mean speed, U_H mean pressure, q_H	100 years	topography factor, E applied to U_0 (turbulence intensity reduced)
AS/NZS 1170.2:2002	Australia/New Zealand	3 s gust speed, V_R	gust speed, $V_{des,0}$	1000 years	topographic multiplier, M_t applied to V_R
ASCE 7-05	U.S.A.	3s gust speed, V	gust pressure, q_z	50 years	topographic factor, K_{zt} applied to V^2
BS 6399-2:1997	Britain	hourly mean speed, V_b	gust speed, V_e	50 years	altitude factor, S_a applied to V_b
EN 1991-1-4: 2005	European CEN nations	10 min mean speed, V_b	gust pressure	50 years	orography factor, $c_o(z)$ applied to V_b
GB 50009-2001	People's Republic of China	10 min mean pressure, w_0	gust pressure, w_k	50 years	a modification factor, η_B , that is multiplied by a terrain factor, μ_z , before application to w_0
HK Code 2004	Hong Kong SAR	3 s gust pressure, q_z	gust pressure, q_z	50 years	topography factor, S_a applied to q_z
IS:875-1987	India	3 s gust speed, V_b	gust speed, V_z	50 years	topography factor, k_3 applied to V_b
NBCC 2005	Canada	hourly mean pressure, q	gust pressure, p	50 years	modified exposure factor, C_e^* applied to q and gust effect factor, C_g^* , so that topography effects are not applied to turbulent fluctuations

and 1 hour respectively, as listed in Table 2. AIJ 2004 and NBCC 2005 carry the mean quantity through the design process, whereas BS 6399-2:1007 and GB 50009-2001 modify the basic wind speed or pressure to a gust wind quantity for design. The majority of standards use a return period of 50 years, with only AIJ 2004 (100 years) and AS/NZS 1170.2:2002 (1000 years) using different return periods.

As the aim of this study is to examine the various provisions related to topography and local wind-induced external pressures, the effects of wind direction, shielding, structural importance and return period were not considered and each of the corresponding multipliers in Eq. (3) were set to unity. As not all standards considered in the current study include exposures for tropical cyclones, the gust wind speed, mean wind speed and turbulence intensity profiles used for each standard calculation were the same as those used for the wind tunnel tests.

Topographic effects were quantified for the test building based on the hillside having a starting point at mean sea level, an average gradient of 0.48 and a height at the crest of 108 m above mean sea level. Topographic multipliers were calculated at building height for each of the nine standards and codes and are presented in Table 3. Also presented in Table 3 is the mean topographic multiplier determined from mean wind speeds measured in the wind tunnel model. For those standards in which a topographic multiplier is applied to a pressure (ASCE 7-05, HK Code 2004, GB 50009-2001, NBCC 2005), the square root of the multiplier is included in Table 3 to allow a direct comparison with multipliers that are applied to wind speed.

It is clear from Table 3 that there are significant differences between the magnitudes of the topographic multipliers determined from the standards and codes, echoing the findings of Holmes *et al.* (2005). For a steep escarpment with a slope whose magnitude is greater than 0.3, BS 6399-

Table 3 Summary of topographic multipliers and external pressure coefficients

Code/Standard	Topographic multiplier	Edge zone (m)	External pressure coefficient			
			windward	leeward	side	edge zone
AIJ 2004 ¹	1.42	1.7	0.9	-1.0	-1.0	-1.3
AS/NZS 1170.2:2002	1.42	3.3	1.0	-0.5	-1.0	-1.3
ASCE 7-05	1.31	1.2	0.9	-0.9	-0.9	-1.8
BS 6399-2:1997	1.31	6.1	0.9	-0.5	-0.8	-1.3
EN 1991-1-4:2005	1.52	6.1	1.0	-0.5	-1.1	-1.4
GB 50009-2001	1.37	-	0.8	-1.0	-1.0	-1.8
HK Code 2004 ²	1.31	4.2	1.0	-1.0	-1.0	-1.4
IS:875-1987	1.32	4.2	0.7	-0.4	-0.7	-1.2
NBCC 2005	1.46	1.7	0.9	-0.9	-0.9	-1.2
wind tunnel test 'without topography'	-	-	0.7	-0.7	-1.0	-1.0
wind tunnel test 'with topography'	1.3	-	0.6	-0.7	-1.2	-1.2

¹AIJ 2004 provides peak external pressure coefficients that have been converted to mean values through the application of a gust effect factor that is based on the turbulence intensity at building height as affected by the topography.

²Values from the Hong Kong Code 2004 correspond to the nett pressure for a nominally sealed building and incorporate internal pressure coefficients of +0.2 and -0.3.

2:1997, EN 1991-1-4:2005, GB 50009-2001, HK Code 2004 and IS:875-1987 stipulate an effective slope of 0.3, similarly for ASCE 7-05 and NBCC 2005 although the corresponding magnitude is 0.25. As the HK Code 2004 has adopted the procedure used in BS 6399-2:1997 it follows that the magnitudes of their respective topographic multipliers should have the same magnitude. AS/NZS 1170.2:2002 sets an upper limit of 0.45, whereas the actual slope of the escarpment is used in AIJ 2004, hence their corresponding topographic multipliers are at the higher end of the range of predicted values. The largest topographic multipliers were determined for EN 1991-1-4:2005 and NBCC 2005, which is consistent with the results presented by Holmes *et al.* (2005) for an escarpment with an average upwind slope of 0.4. The agreement between the topographic multiplier determined from the wind tunnel tests and AS/NZS 1170.2:2002, ASCE 7-05, BS 6399-2:1997, GB 50009-2001, HK Code 2004 and IS:875-1987 do provide some further justification for the use of an upper limit for the effective slope.

A further complication is that some standards apply topographic multipliers to gust design speeds and pressures and some are mean topographic multipliers. Of the standards considered in this study, the assessments of topographic effects in AIJ 2004, BS 6399-2:1997, EN 1991-1-4:2005 and NBCC 2005 recognize that wind flows over large topographical features, such as the hillside upon which the HKUST test building is located, have a significant effect on the mean wind speed whereas the fluctuating components of wind speed remain largely unaffected. The procedure in BS 6399-2:1997 deliberately applies the topographic multiplier to the basic mean wind speed prior to its modification to a design gust wind speed, recognizing that this provides a more accurate treatment of the effects of topography. Similarly, the procedure in EN 1991-1-4:2005 applies an orography factor to the mean wind speed, but not to the turbulence intensity, to determine a peak velocity pressure. In NBCC 2005, corrections are made to the gust effect factor so that topography induced speed-up effects are applied to the mean wind speed and not to the turbulent fluctuations. The HK Code 2004 applies the same topographic multiplier as BS 6399-2:1997 but to the design gust wind pressure.

The effects of topography on turbulence are addressed in AIJ 2004 by determining a separate topography factor for the standard deviation of the fluctuating wind speed, E_i , which is then divided by the mean topographic multiplier and applied to the turbulence intensity. For the current study, the turbulence intensity topography factor determined using this technique is 0.83 from which the modified turbulence intensity has a calculated value of around 19%. This compares very well with the turbulence intensity that was measured in the wind tunnel model directly above the building site but with the building removed, which is also approximately 19%.

6.2 External pressure coefficients

In the determination of peak pressures for the design of cladding, components or local structural elements using the standards and codes considered in this study, basic pressure coefficients, C_p , are modified by the application of several factors to determine appropriate external pressure coefficients, C_{pe} , that are also sometimes called aerodynamic shape factors. As shown in Eq. (4), the factors that are relevant to cladding typically include an area reduction factor, K_a , a local pressure factor, K_l , and a permeable cladding factor, K_p .

$$C_{pe} = C_p K_a K_l K_p \quad (4)$$

In the current study, the tributary area is assumed to be less than 10 m² and the cladding is

assumed to be impermeable, therefore, the factors K_a and K_p are unity. The magnitudes of the local pressure factors vary across the standards considered here, as do the definitions of the various pressure zones.

A summary of external pressure coefficients determined from the different design standards and wind codes is presented in Table 3 for the windward, leeward and side building faces, and in recommended edge zones for the test building. In order to allow a direct comparison between each of the standards, the peak pressure coefficients included in AIJ 2004 have been adjusted by a gust effect factor that is based on the turbulence intensity of 19% calculated above.

Table 3 demonstrates the significant differences between the various standards and codes, in the large range of magnitudes of the external pressure coefficients, particularly for the leeward building face and edge zones, and with the size of the edge zone varying from 1.7 m up to 6.1 m. Those differences between the standards would be exacerbated when the external pressure coefficients are combined with design wind speeds that include the topographic multipliers listed in Table 3.

Mean pressure coefficients measured in the wind tunnel tests at relevant pressure-tap locations are also included in Table 3 for comparison with the external pressure coefficients from the standards. Some of the differences between the external pressure coefficients of the standards and the test building are likely to be due to the slightly irregular building shape and localized effects caused by the surface features of the test building that were included in the wind tunnel model. Although at first glance, the HK Code 2004 would appear to provide the closest agreement with the wind tunnel test results, it is necessary to note that its corresponding external pressure coefficients are equivalent to total pressure coefficients that already include internal pressure allowances assuming the building has no dominant openings.

In general, the majority of the standards would be likely to adequately predict the windward wall pressures experienced by the building. However, apart from AS/NZS 1170.2:2002, ASCE 7-05 and EN 1991-1-4:2005, the design standards and wind codes considered in this study tended to underestimate pressures in general areas on the side face that are outside of the edge zone. This is attributed to the effects of the building form and detail that caused relatively consistent peak suction pressures over the front half of the building's side face. From a practical perspective, this may not amount to a serious concern if a single "worst-case" negative pressure is specified for cladding design, but implies that the building form and details did modify the flow regime.

7. Conclusions

Wind tunnel model tests were conducted on a nine storey, medium-rise building located on a hillside that is typical of residential buildings in coastal areas in Hong Kong. It was found that the distribution of external mean wind pressure coefficients for the 'without topography' test are in quite close agreement with the mean pressure distributions that were determined from the 'with topography' configuration when they are normalized by the mean wind speed at building height. This justifies the typical quasi-steady type approach commonly adopted by international design standards and wind codes.

Significant differences were found between the magnitudes of the topographic multipliers determined from the standards and codes. This is attributed to differences in the way the topographic multiplier is determined and applied. For steep slopes, there is some further justification for the use of an upper limit for the effective slope of a topographical feature. Where topographic multipliers are

applied to gust wind speeds, the effects of topography on turbulence intensity can be more accurately determined than many standards presently do.

While the majority of the standards are likely to adequately predict pressures on windward faces, there are large differences in the magnitudes and definitions of pressure zones on side and leeward faces. The general over-predictions of suction pressure coefficients in edge zones are probably consistent with the aim of most design standards to provide design data that errs on the conservative side.

The determination of wind-induced pressures around buildings in locations dominated by significant topography would benefit from a detailed study of the effects of flow modifications/amplifications associated with the topography, and the adoption of suitably modified wind flow simulation in the pressure model tests.

Acknowledgements

This research project is funded by a Research Grants Council of the Hong Kong Special Administrative Region, China (Project HKUST 6293/03E). The contributions of Mr. Desmond Hui, Mr. Jie Yuan and Mr. Martin Ko are gratefully acknowledged.

References

- American Society of Civil Engineers (2005), *Minimum design loads for buildings and other Structures*, SEI/ASCE 7-05, ASCE, Reston, VA.
- Architectural Institute of Japan (2004), *Recommendations for loads on buildings*, (in English), AIJ, Tokyo.
- British Standards Institution (1997), *Loading for buildings – Part 2: Code of practice for wind loads*, BS 6399-2, BSI, London, UK.
- Buildings Department (2004), *Code of Practice on Wind Effects in Hong Kong*, The Government of the Hong Kong Special Administrative Region, Hong Kong.
- China Architecture and Building Press (2006), *Load code for the design of building structures*, China National Standard, GB 50009-2001, CABP, Beijing, China.
- Chock, G.Y.K. and Cochran, L. (2006), Erratum to “Modeling of topographic wind speed effects in Hawaii”, *J. Wind Eng. Ind. Aerod.*, **94**(3), 173-187.
- C.E.N. (European Committee for Standardization) (2005) *Eurocode 1: Actions on structures - General actions - Part 1-4: Wind actions*, prEN 1991-1-4.6, C.E.N., Brussels.
- Glanville, M.J. and Kwok, K.C.S. (1997), “Measurements of topographic multipliers and flow separation from a steep escarpment: Part II. Model-scale measurements”, *J. Wind Eng. Ind. Aerod.*, **69-71**, 893-902.
- Holmes, J.D. (2007), *Wind loading of structures*, 2nd Edition, Taylor and Francis Group, London, UK.
- Holmes, J.D., Banks, R.W. and Paevere, P. (1997), “Measurements of topographic multipliers and flow separation from a steep escarpment. Part I. Full scale measurements”, *J. Wind Eng. Ind. Aerod.*, **69-71**, 885-892.
- Holmes, J.D., Baker, C.J., English, E.C. and Choi, E.C.C. (2005), “Wind structure and codification”, *Wind Struct.*, **8**(4), 235-250.
- Indian Standards Institution (1987), *Code of practice for design loads (other than earthquake) for buildings and structures, Part 3 Wind Loads*, Second Revision, Indian Standard, IS 875: Part 3, India.
- Kondo, K., Tsuchiya, M. and Sanada, S. (2002), “Evaluation of effect of micro-topography on design wind velocity”, *J. Wind Eng. Ind. Aerod.*, **90**(12-15), 1707-1718.
- Letchford, C.W., Holmes, J.D., Hoxey, R. and Robertson, A. (2005), “Wind pressure coefficients on low-rise structures and codification”, *Wind Struct.*, **8**(4), 283-294.
- Miller, C.A. and Davenport, A.G. (1998), “Guidelines for the calculation of wind speed-ups in complex terrain”,

- J. Wind Eng. Ind. Aerod.*, **74-76**, 189-197.
- National Research Council of Canada (2005), *User's Guide – NBC 2005 Structural Commentaries (Part 4 of Division B)*.
- St. Pierre, L.M., Kopp, G.A., Surry, D. and Ho T.C.E. (2005), “The UWO contribution to the NIST aerodynamic data base for wind loads on low buildings: Part 2. Comparison of data with wind load provisions”, *J. Wind Eng. Ind. Aerod.*, **93**, 31-59.
- Standards Australia/Standards New Zealand (2002), *Australia/New Zealand Standard, Structural design actions Part 2: Wind actions*, AS/NZS 1170.2.
- Uematsu, Y. and Isyumov, N. (1999), “Wind pressures acting on low-rise buildings”, *J. Wind Eng. Ind. Aerod.*, **82**(1-3), 1-25.
- Weng, W., Taylor, P.A. and Walmsley, J.L. (2000), “Guidelines for airflow over complex terrain: model developments”, *J. Wind Eng. Ind. Aerod.*, **86**(2-3), 169-186.
- Zhang, X. (2003), “Introduction and some observations on 2002 Chinese Wind Load Code”, *Proceedings of the 11th International Conference on Wind Engineering*, Lubbock, Texas, USA, June.

JH